Deeply Virtual Compton Scattering at Jefferson Lab

Franck Sabatié

SPhN/Irfu, CEA, Centre de Saclay, 91191 Gif sur Yvette, France

The Generalized Parton Distribution framework was introduced in the late 90's and describes the nucleon in a revolutionary way, correlating the information from both momentum and transverse position space into experimentally accessible functions. After a brief introduction, this article reviews the Jefferson Lab 6 GeV measurements of Deeply Virtual Compton Scattering in Halls A and B, which give a unique access to Generalized Parton Distributions (GPD). The second part of this article reviews the Jefferson Lab 12 GeV upgrade in general terms, and then focuses on the GPD program in Halls A and B.

1 Introduction

The nucleon electromagnetic structure is still a challenge to modern day physicists after more than 50 years of experimental scrutiny. The nucleon, which appeared to be an elementary particle at first, turned out to have a complicated structure, described in turns by Form Factors (FF) measured in elastic scattering, and Parton Distribution Functions (PDF) measured in Deep Inelastic Scattering (DIS). With the advent of higher energy and higher luminosity accelerators, coupled to high resolution and/or acceptance detectors, it is possible to extend the landscape of hard scattering from inclusive processes such as DIS to exclusive processes, which contain a wealth of new information about the nucleon structure. Similar to parton distributions for DIS, the Generalized Parton Distributions (GPD) which can be obtained through the study of Deep Exclusive Scattering (DES) processes contain information on the quark/antiquark and gluon correlations, and more specifically on both the transverse spatial and longitudinal momentum dependences.

Generalized Parton Distributions not only contain the usual Form Factors and Parton Distribution functions, but using the fully correlated transverse position - momentum information, they can be used to provide 2D tomographic images of the nucleons [1, 2], or even genuine 3D images using their full kinematical dependence [3]. Last but not least, GPD's will allow us to quantify the role of the quark angular orbital momentum in the nucleon spin sum rule [4], which is an open issue since polarized DIS was first investigated.

Jefferson Lab has been a key contributor in the field of GPD's since 2001, especially studying the Deeply Virtual Compton Scattering (DVCS) process. The rest of this article will review the DVCS Jefferson Lab measurements and the future prospects after the 12 GeV upgrade.

2 Deeply Virtual Compton Scattering to access GPD's

About 10 years ago, Mueller, Ji, Radyushkin and others [5, 6, 7, 8, 9] showed that the Deeply Virtual Compton Scattering reaction $\gamma^* p \to \gamma p$ can, in the Bjorken limit, be factorized into a hard scattering kernel and a non-perturbative part, containing information about the electromagnetic structure of the nucleon parametrized into Generalized Parton Distributions. This factorization of the DVCS reaction is represented in Fig.1, where the virtual photon scatters on a single quark, which almost instantly re-emits a real photon. The quark is then inserted back into the nucleon, which is kept intact. In kinematical terms, this factorization is valid when the virtuality of the incoming photon is large ($Q^2 = -q^2$, with q the virtual photon 4-vector) but the transfer to the nucleon small compared to this scale ($-t << Q^2$). The soft structure of the nucleon is parametrized at twist-2 level by four GPD's: E, H, $\widetilde{E}$ and $\widetilde{H}$.
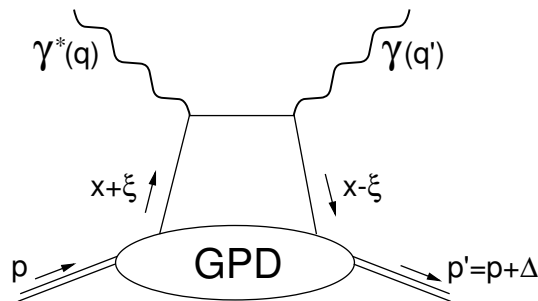
Figure 1: Handbag diagram to the DVCS process. See text for definition of variables.

DVCS is accessible through the electroproduction of real photons $ep \to ep\gamma$. This reaction has a very interesting feature: the real photon can either be emitted by the proton (DVCS) or from one of the electron lines (Bethe-Heitler or BH). Both processes are not distinguishable, therefore they interfere at the amplitude level. By measuring the difference of cross sections for opposite lepton helicities or opposite target polarization, one is sensitive to the interference term alone, which is basically the product of the DVCS amplitude imaginary part by the BH amplitude. This is especially useful at moderate energy at Jefferson Lab since Bethe-Heitler is strong in these kinematics and the cross section difference is therefore sizeable. The difficulties of such measurements lie in the need for exclusivity, which usually means the detection of the three-particle final state, as well as the low cross section which can be compensated by high luminosity and/or acceptance.

3 Jefferson Lab DVCS 6 GeV measurements

3.1 Hall A

The E00-110 experiment in Hall A took data in the fall 2004 with 5.75 GeV electron beam energy impinging on a 15 cm liquid hydrogen target. The experiment was the first ever dedicated DVCS experiment worldwide, its main goal was to check the factorization in the DVCS reaction, by means of a Q^2 scaling scan at fixed x_B. This experiment used the Hall A High Resolution Spectrometer (HRS) to detect the scattered electron, a 132-block lead-fluoride calorimeter to

detect the emitted photon and an array of out-of-plane scintillator blocks to detect the recoil proton. An important feature of this experiment was the high 10^{37} cm^{-2}s^{-1} luminosity which allowed very accurate measurements of the helicity dependent cross sections. The cross section difference and the total cross section are shown on Fig.2 (left) as a function of ϕ, the angle between the leptonic and hadronic planes [10]. The Q^2 dependence of the $\sin \phi$ coefficient is shown on Fig. 2 (right) and shows no visible dependence, which is a good indication the handbag diagram is indeed the dominant process in DVCS even at rather low Q^2. The analysis of the total cross section in terms of GPD's is made more complicated by the fact that one cannot disentangle the DVCS^2 terms from the interference contributions with a simple fit to the data. Only a Rosenbluth-type extraction, using the different energy dependences of these contributions would allow for a complete extraction.
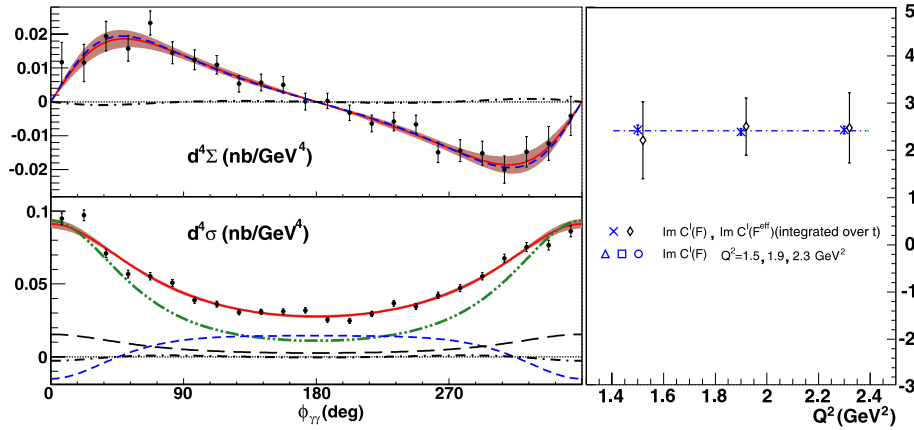
Figure 2: Left: Cross section difference (top) and total cross section (bottom) for $x_B = 0.36$, Q^2=2.3 GeV^2 and $-t$=-0.28 GeV^2. Right: Scaling of the $\sin \phi$ and $\sin 2\phi$ coefficients indicating a handbag dominance. Data and more information can be found in [10].

The E03-106 experiment in Hall A immediately followed E00-110 and took data on a liquid deuterium target in order to extract information on neutron GPD's. Indeed, by subtracting the proton contribution to the deuterium, up to nuclear effects included in systematics, one can extract the cross section difference on the neutron, from which the $\sin \phi$ coefficient is shown on Figure 3 (left, bottom). The collaboration compared their results with the VGG calculations [11] in order to constrain the total angular momentum carried by the u and d quarks through the parametrization of the GPD E [12], as shown on Figure 3 (right). Even though this extraction is highly model dependent, it is a step in the right direction and shows clear potential with more data and other more realistic models. The deuteron $\sin \phi$ coefficient is also shown on Figure 3 (left, top).

3.2   Hall B

The Hall B CLAS collaboration ran the E1-DVCS experiment in 2005 using a 5.77 GeV electron beam impinging on a 2.5 cm-long liquid hydrogen target. In contrast with the Hall A experiments, the operating luminosity was much lower at 2×10^{34} cm^{-2}s^{-1}, but was still a record in the open geometry large acceptance CLAS spectrometer. The standard equipment of this
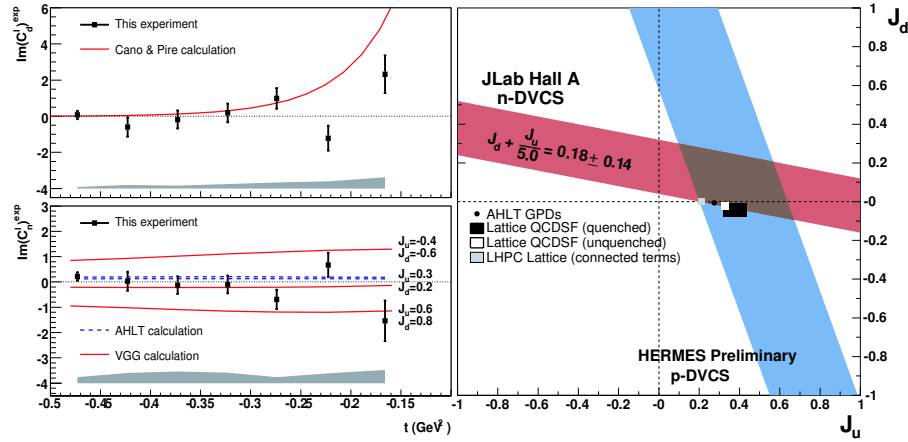
Figure 3: Left top: Coherent deuterium DVCS $\sin\phi$ coefficient as a function of t along with Cano-Pire model [13]. Left bottom: Neutron DVCS $\sin\phi$ coefficient as a function of t along with VGG model. The VGG input parameters for the GPD E are J_u and J_d in this model. Right : Resulting constraint on J_u and J_d. Data and more information can be found in [12].

spectrometer was complemented in this experiment by a new electromagnetic calorimeter (Inner Calorimeter, IC) located 55 cm downstream from the target, in order to detect 1 to 5 GeV photons emitted between $4.5°$ and $15°$ with respect to the beam direction. This calorimeter was built of 424 tapered lead tungstate crystals, 16 cm long and with an average cross sectional area of 2.1 cm^2, read out with avalanche photodiodes and associated low-noise preamplifiers.

The analysis of the data consisted in selecting a clean sample of triple coincidence events ($ep\gamma$) and using a set of exclusivity cuts, making sure no other particles were present in the reaction. In spite of this selection, a contamination of events originating from the $ep \to ep\pi^0$ reaction, followed by the subsequent asymmetric decay of the neutral pion, is always possible. It was estimated using π^0 events where both photons are recorded and a Monte-Carlo simulation to correct for the ratio of acceptance for 2-detected photons to 1-detected photons events. The data are then divided into bins in Q^2, x_B, t and ϕ and the beam spin asymmetry is calculated for each bin, plotted as a function of ϕ as shown on Fig. 4 [14], along with the kinematical coverage in Q^2 and x_B. These data represent the largest data set on DVCS to date and they are compared to a number of models and GPD parametrizations such as VGG and others [11, 15, 16, 17, 18].

The only available data on DVCS using a longitudinaly polarized proton target at Jefferson Lab are from non-dedicated data in Hall B [19]. The asymmetry A_{UL} shown in Figure 5 is dominated by the $\sin\phi$ term while the $\sin 2\phi$ term is compatible with zero. As expected, the measured asymmetry is consistent with predictions of a large contribution from the GPD $\widetilde{H}$.
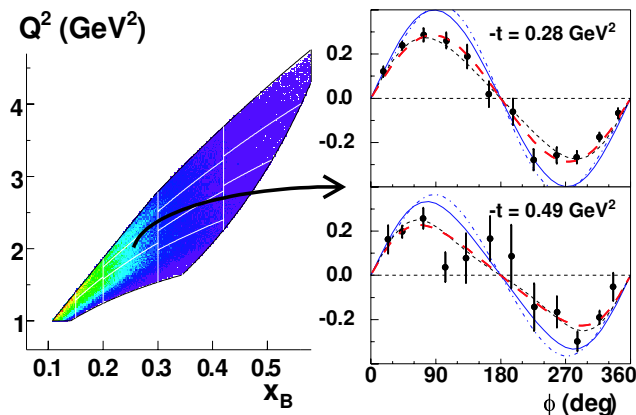
Figure 4: Left: kinematic coverage and binning in the (x_B, Q^2) space. Right: $A(\phi)$ for 2 of the 62 (x_B, Q^2, t) bins, corresponding to $x_B = 0.249$, $Q^2 = 1.95$ GeV^2, and two values of t. Data and more information can be found in [14].

4 The DVCS program at 11 GeV

4.1 The Jefferson Lab 12 GeV Upgrade

The accelerator portion of the Upgrade is straightforward and utilizes the existing tunnel without changing the basic layout of the accelerator. There are four main changes: additional acceleration in the linacs, stronger magnets for the recirculation, an upgraded cryoplant, and the addition of a tenth recirculation arc. The extra arc permits an additional "half pass" through the accelerator to reach the required 12 GeV beam energy, followed by beam transport to Hall D that will be added to support the meson spectroscopy initiative.

The equipment planned for the Upgrade project takes full advantage of apparatus developed for the present program. In two of the existing halls new spectrometers are added and/or present equipment upgraded to meet the demands of the 12 GeV program. Then a new hall, Hall D, will be added to support the meson spectroscopy program. In Hall A, the Upgrade will only add 11 GeV capability to the beamline and will allow for special setup experiments. In Hall B, the CEBAF Large Acceptance Spectrometer (CLAS), which was designed to study multiparticle, exclusive reactions with its combination of large acceptance and moderate momentum resolution, will be upgraded to CLAS12 and optimized for studying exclusive reactions and especially the investigation of GPD's. In Hall C a new, high-momentum spectrometer (the SHMS, Super-High- Momentum Spectrometer) will be constructed to support high-luminosity experiments detecting reaction products with momenta up to the full 11 GeV beam energy. Finally, in Hall D, a tagged coherent bremsstrahlung beam and solenoidal detector will be constructed in support of a program of gluonic spectroscopy.

4.2 The 11 GeV DVCS program in Hall A

The proposal PR12-06-114, accepted by the PAC30 of Jefferson Lab, will measure the $ep \rightarrow ep\gamma$ cross sections at fixed x_B for Q^2 up to 9 GeV^2, using a similar (but upgraded) equipment to
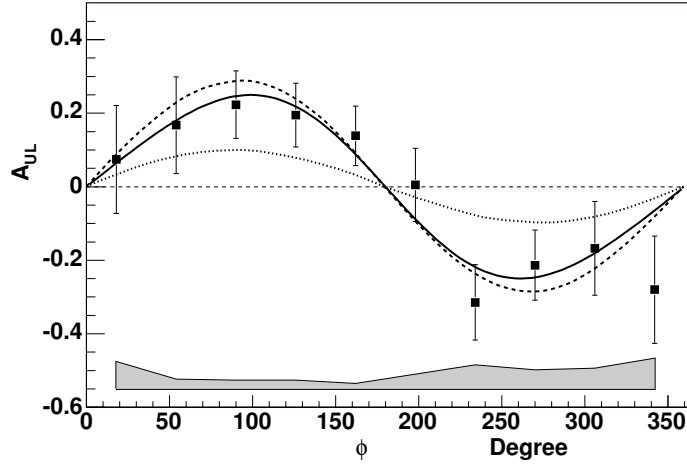
Figure 5: The azimuthal angle ϕ dependence of the target-spin asymmetry for exclusive electroproduction of photons. The dashed curve is the full VGG model prediction. The dotted curve shows the asymmetry when $\widetilde{H} = 0$. The solid curve is a simple fit to the data. Data and more information can be found in [19].

the 6 GeV experiment described earlier. This will determine with what precision the handbag amplitude dominates over the higher twist amplitudes. Using several beam energies, it will be able to fully separate the total cross section among its different contributions, especially DVCS^2, the size of which is mostly unknown. It will also extract superpositions of Compton Form Factors (CFFs). The Q^2 vs x_B domain as well as simulated data for one of the highest Q^2 setting is shown on Fig. 6. In addition, this experiment will measure the $ep \rightarrow ep\pi^0$ cross section in the same kinematics as DVCS and even perform a L-T separation of this cross section for the first time.
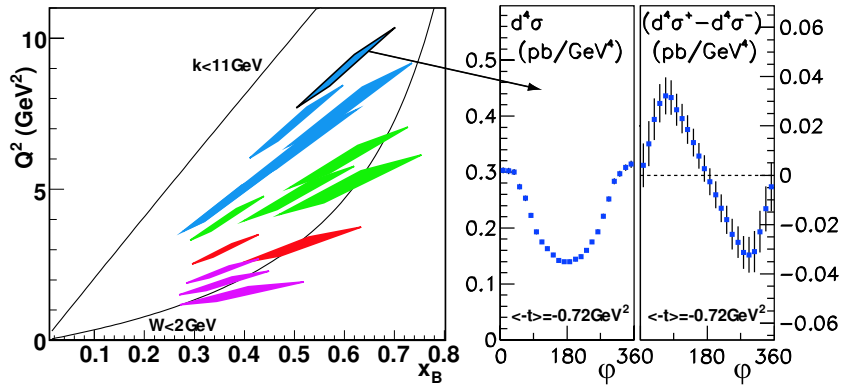
Figure 6: Left: Hall A 11GeV Q^2 vs x_B kinematical coverage: Right: simulated data for the kinematics highlighted on the left.

4.3 The 11 GeV DVCS program in Hall B

The proposal PR12-06-119, accepted by the PAC30 of Jefferson Lab, consists in two separate experiments for a total of 200 days of beam time. The first is a measurement of the DVCS beam spin asymmetries from an unpolarized liquid hydrogen target, and therefore mostly sensitive to the GPD H. The second experiment is dedicated to measuring DVCS target spin asymmetries using a longitudinally polarized target, which is mostly sensitive to the GPD $\widetilde{H}$. These proposals will extend the previous CLAS measurements up to $Q^2 = 9$ GeV^2, using a high 10^{35} cm^{-2}s^{-1} luminosity as well as the augmented CLAS12 detector, including the inner calorimeter already used in the 6 GeV experiment. Simulated data for the beam spin asymmetries are presented on Fig. 7.
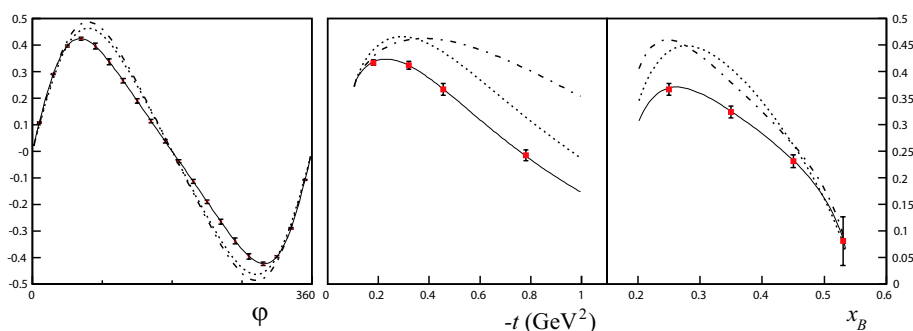
Figure 7: Left : Simulated data for CLAS12 DVCS Beam Spin Asymmetry as a function of ϕ. Middle and right: $A(90°)$ as function of t and x_B as well as curves from [11].

5 Summary

The first 6 GeV dedicated experiments at Jefferson Lab published their data two to three years ago and already, we are challenged to understand their meaning and extract reliable Generalized Parton Distribution information from them. As expected, Deeply Virtual Compton Scattering seems to be scaling early as proved by the Hall A experiment, and constitutes as promised the golden process to access GPD's at moderate energies and Q^2. An enormous amount of data in the valence quark region is now available from Hall B in terms of the A_{LU} asymmetry, soon to be extended to absolute cross section. Along with the very accurate Hall A data, this will constitute a benchmark for GPD parametrization and modelling and keep the community busy until the Jefferson Lab 12 GeV upgrade. The expected data for this second generation of experiments in Halls A and B will undoubtedly unravel for the first time the precise 3-dimensional structure of the nucleon.

References

[1] Matthias Burkardt. Impact parameter space interpretation for generalized parton distributions. *Int. J. Mod. Phys.*, A18:173–208, 2003.

[2] M. Diehl. Generalized parton distributions in impact parameter space. *Eur. Phys. J.*, C25:223–232, 2002.

[3] Andrei V. Belitsky, Xiang-dong Ji, and Feng Yuan. Quark imaging in the proton via quantum phase-space distributions. *Phys. Rev.*, D69:074014, 2004.

[4] Xiang-Dong Ji. Gauge invariant decomposition of nucleon spin. *Phys. Rev. Lett.*, 78:610–613, 1997.

[5] Dieter Mueller, D. Robaschik, B. Geyer, F. M. Dittes, and J. Horejsi. Wave functions, evolution equations and evolution kernels from light-ray operators of QCD. *Fortschr. Phys.*, 42:101, 1994.

[6] Xiang-Dong Ji. Deeply-virtual compton scattering. *Phys. Rev.*, D55:7114–7125, 1997.

[7] A. V. Radyushkin. Scaling limit of deeply virtual compton scattering. *Phys. Lett.*, B380:417–425, 1996.

[8] John C. Collins and Andreas Freund. Proof of factorization for deeply virtual Compton scattering in QCD. *Phys. Rev.*, D59:074009, 1999.

[9] M. Diehl, T. Feldmann, R. Jakob, and P. Kroll. Linking parton distributions to form factors and compton scattering. *Eur. Phys. J.*, C8:409–434, 1999.

[10] C. Munoz Camacho et al. Scaling tests of the cross section for deeply virtual Compton scattering. *Phys. Rev. Lett.*, 97:262002, 2006.

[11] K. Goeke, Maxim V. Polyakov, and M. Vanderhaeghen. Hard exclusive reactions and the structure of hadrons. *Prog. Part. Nucl. Phys.*, 47:401–515, 2001.

[12] M. Mazouz et al. Deeply Virtual Compton Scattering off the neutron. *Phys. Rev. Lett.*, 99:242501, 2007.

[13] F. Cano and B. Pire. Deeply virtual Compton scattering on the deuteron. *Nucl. Phys.*, A711:133–138, 2002.

[14] F. X. Girod et al. Deeply Virtual Compton Scattering Beam-Spin Asymmetries. *Phys. Rev. Lett.*, 100:162002, 2008.

[15] Maxim V. Polyakov and Marc Vanderhaeghen. Taming Deeply Virtual Compton Scattering. 2008.

[16] M. Guidal. A fitter code for Deep Virtual Compton Scattering and Generalized Parton Distributions. *Eur. Phys. J.*, A37:319–332, 2008.

[17] H. Moutarde. Extraction of the Compton Form Factor H from DVCS measurements at Jefferson Lab. *Phys. Rev. D*, 79:094021, 2009.

[18] Kresimir Kumericki and Dieter Muller. Deeply virtual Compton scattering at small x_B and the access to the GPD H. 2009.

[19] S. Chen et al. Measurement of deeply virtual Compton scattering with a polarized proton target. *Phys. Rev. Lett.*, 97:072002, 2006.